MRE2019_2

by Leny Yuliati

Materials Research Express

PAPER

CrossMark

Comparison study on molybdena-titania supported on TUD-1 and TUD-C synthesized via sol-gel templating method: Properties and catalytic performance in olefins epoxidation

Yee Khai Ooi[1], Faisal Hussin[1], Leny Yuliati[2,3] and Siew Ling Lee[1,2]

[1] Department of Chemistry, Faculty of Science, Universiti Teknologi Malaysia, 81310 Johor Bahru, Johor, Malaysia
[2] Centre for Sustainable Nanomaterials, Ibnu Sina Institute for Scientific & Industrial Research, Universiti Teknologi Malaysia, 81310 Johor Bahru, Johor, Malaysia
[3] Ma Chung Research Center for Photosynthetic Pigments, Universitas Ma Chung, Malang 65151, Indonesia

E-mail: sllee@ibnusina.utm.my

Abstract

A direct comparison between nanostructured Technische Universiteit Delft-1 (TUD-1) and Technische Universiteit Delft-Crystalline (TUD-C) as catalyst supports for molybdenum doped titania catalysts was carried out. The characterizations results showed that TUD-1 is a mesoporous amorphous silicate material with high surface area and porosity. Meanwhile, TUD-C is an ordered mesoporous crystalline aluminosilicate matters featured high acidity. In fact, TUD-C was obtained from the modification of TUD-1 with the addition of aluminium isopropoxide as the zeolite precursor. The catalytic testing demonstrated TUD-1 supported 1 mol% molybdena doped titania was inactive for epoxidation of 1,2-epoxyoctane and showed moderate activity (18%–21% conversion yield) and selectivity (approximately 70%) in epoxidation reaction of 1,2-epoxycyclohexane (0.51 mmol) and styrene oxide (1.25 mmol). Meanwhile, TUD-C supported 1 mol% molybdena doped titania achieved remarkably higher conversion yield for 1,2-epoxyoctane (2.7 mmol), 1,2-epoxycyclohexane (4.8 mmol) and styrene oxide (6.2 mmol) respectively with 100% selectivity towards all 3 analytes under ambient condition with constant stirring. The results strongly indicated that high Brønsted and Lewis acidic sites existed within the TUD-C framework is the key factor for the exceptional oxidative capabilities for molybdena-titania catalysts.

1. Introduction

Catalytic supporting constituents have been the significant part and predominantly used to assist numerous chemical applications such as conversion of olefins, production of fine chemical, synthesis of polymer, pharmaceutical and drug delivery [1]. Usually, titanosilicate (TS-1) [2], huge surface area mesoporous silicate supporting material for example the Mobil Composition of Matters (MCM), Santa Barbara Amorphous (SBA), mesoporous silica nanoparticles (MSN) and silica aerogel are used as supporting materials [3–5]. Since these materials are playing crucial roles in various applications, nonetheless, the present industrial approaches are incompetent to attain adequate results because of small produce and discernment, and the materials employed are typically vastly inert with costly synthesis processes. Hence, numerous scientists already reported of utilizing transition metal oxides catalytic agent due to its high efficacy and catalytic performance [6, 7]. Amongst, molybdena is extensively accounted as efficient heterogeneous catalyst [6]. In spite of the efficiency by homogeneous catalytic substance, managerial difficulties as gruelling partition still existing. Thus, application of heterogeneous catalytic substance particularly TiO_2 has enticed laborious consideration from scientists because of its low cost and toxicity. It was recounted that Mo–TiO_2 was an imminent heterogeneous catalyst [7]. Nevertheless, catalyst agglomeration has resulted low surface area (5 $m^2 g^{-1}$) of the catalyst, thus restricting the catalytic effectiveness. For that reason, supporting material application for enriched dispersal of catalytically

reactive sites is endorsed. Regrettably, catalytic performance and selectivity of the supporting substances are still substantially unsatisfactory. Zeolitic material with mesoporosity featuring miscellaneous frameworks was recommended by means of potential answer for problematic refinement. Attributable to the immense acidic sites and great surface area (>1500 m^2 g^{-1}), zeolitic material was applied catalytically for numerous reactions. Yet, microporosity of zeolitic material had occasioned porosity obstruction, therefore limiting the applicability for handling of huge reactants [8].

The above-mentioned liabilities could be resolute via hone-tuned porosity of zeolite by means of sol-gel soft templating method. Furthermore, fine-tuning mesopores may perhaps remain as the key characteristic to achieve optimum diffusivity in gasoline catalytic cracking [9]. Zeolite Socony Mobil-Five (ZSM-5) with Modernite Framework Inverted (MFI) structure was nominated as the highly appropriate catalytic supporting material due to its excellent activity, adaptability and high compatibility [10]. Many researches have been engrossed in assimilation of well-ordered mesoporosity to zeolitic structure. Technische Universiteit Delft-Crystalline (TUD-C) is a crystalline aluminosilicate with mesoporosity that featured MFI framework structure of zeolitic material assimilated inside silicate with mesoporous arrangement. Predominantly, TUD-C's porosity can be straightforwardly optimized via steam-assisted hydrothermal approach [11]. As the matter of state, TUD-C is an additional single-approach alteration derived of Technische Universiteit Delft-1 (TUD-1), which is mesoporous silicate with immense surface area and porosity; hence could be produced from a modest approach by adding in alumina precursor. Beforehand reports stated that a zeolitic material with ordered micro-mesoporous arrangement that symptomatically affiliated to TUD-1 is achieved via orthodox steam-reforming treatment. That material demonstrated excellent catalyst activity comparing mutually unstructured zeolitic material and conventional ZSM-5 as catalyst regarding large materials [12]. Telalovic *et al.* stated that TUD-1 with a 3D foam-akin mesoporosity was straightforwardly perceived featuring excellent flexibility. TUD-1 can be straightforwardly assimilated with various transition metal oxides, performing miscellaneous catalytically applications. With catalytic integration of dual-metallic TUD-1, synergy between Lewis and Brønsted acidities can be introduced. Additionally, efficacious utilizations in acid-, redox-, and photocatalysis already confirmed the efficiency of TUD-1 as outstanding catalytic support, conveying innovative applications [13]. TUD-C that contrives from TUD-1 with higher mesoporosity and acidity could be a potential supporting material. However, TUD-C as catalytic supporting material is still scarce; several of its properties are remained unfamiliar. Hence, supplementary exploration on its application as catalyst supporting material is essential.

In recent times, application of both Technische Universiteit Delft-1 (TUD-1) and Technische Universiteit Delft-Crystalline (TUD-C) as catalyst support in Cr doped TiO$_2$ photocatalysts and Mo doped TiO$_2$ catalysts, respectively have been reported and discussed in previous works [14–16]. The improved catalytic performance suggested that TUD-1 and TUD-C were auspicious catalyst supporting materials. In this work, characteristically comparison between TUD-1 and TUD-C was inspected and the practicability of TUD-1 and TUD-C as catalyst support of 1 mol% molybdena doped titania, Mo doped TiO$_2$ catalyst for epoxidation of olefins was investigated. The catalytic attainment of these materials in numerous types of olefins epoxidation was reported.

2. Experimental

2.1. Synthesis of catalysts

Mo doped TiO$_2$ was synthesized via sol-gel approach from foregoing research [15]. The solution was readied via addition of titanium tetraisopropoxide (TTIP, $>99\%$), ethanol (EtOH, $>99\%$) and acetylacetone (acac, 97%) conferring to ratio of 1TTIP: 100EtOH: 2acac. All reagents used were from Sigma-Aldrich with analytical grade. In the meantime, molybdena precursor (ammonium molybdate) was dissolved using ethanol as solvent. Mo dopant (1 mol%) was drop-wisely added into solution whilst stirring for 2 h. Removal of solvent was done at 353 K and overnight drying at 383 K, consequently calcination at 823 K for attainment of Mo–Ti.

TUD-1 was produced via sol-gel method followed by steam-assisted hydrothermal treatment together with triethanolamine (TEA) and tetraethylammonium hydroxide (TEAOH) as the structure directing and mesopore templating agent. The synthesis accorded to molar ratio of 1TEOS: 0.5TEA: 0.1TEAOH: 11H$_2$O. The homogeneous mixture was then aged at 298 K for 24 h, materializing solid gel. Sample was relocated inside autoclave, went through 10 h hydrothermal treatment at 403 K and drying at 373 K, successively calcination in air for 6 h at 873 K to eliminate carbon-based constituents. For the production of molybdena-titania supported on TUD-1, molar ratio Si/Ti = 30, 1 mol% Mo–Ti synthesized beforehand was inserted into TUD-1 solution with affixed molar ratio Si/Ti = 30 before underwent evaporation. The sample was represented by Mo–Ti@TUD-1.

TUD-C was synthesized via a homogeneous mixture involving water, triethanolamine, TEA 97 wt%, tetraethylammonium hydroxide, TEAOH 2 M in water, tetraethyl orthosilicate, TEOS 98 wt%, and aluminum
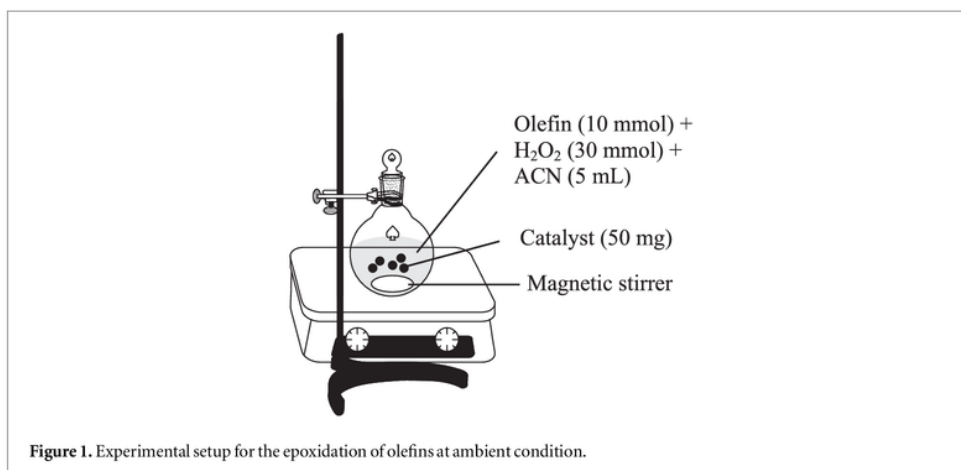
Figure 1. Experimental setup for the epoxidation of olefins at ambient condition.

isopropoxide, Al(iPro)$_3$ 97% according to molar ratio of 1TEOS: 10Al$_2$O$_3$: 0.5TEA: 0.1TEAOH: 0.3NaOH: 11H$_2$O [16]. The mixture was assigned for evaporation at room temperature overnight to acquire solid gel. After that, solid gel was grounded. The fine-powdery product was transmitted inside autoclave and went through 10 h of hydrothermal treatment at 403 K subsequently dried at 373 K. Calcination was done in air for 6 h at 873 K to eradicate carbon-based components. For the production of Mo–Ti@TUD-C with molar ratio Si/Al = 10, 1 mol% Mo–Ti synthesized earlier was added into the TUD-C solution with affixed Si/Ti molar ratio = 30 prior aging process. Obtained sample was represented by Mo–Ti@TUD-C. Samples Mo–Ti, TUD-1 and TUD-C were also produced for comparison purpose.

2.2. Characterization

All the synthesized products were characterized with powder x-ray diffraction (XRD) analysis for crystalline formation and phase pureness. XRD analysis was performed via powder Bruker Advance D8 diffractometer (40 kV, 40 mA) fitted with CuK$_a$ (k = 0.154 nm) incident beam monochromator. Step size was 0.0175° with the intervals of 8 s. Spectra of Fourier transform infrared (FTIR) were detailed using Nicolet iS10 spectrometer via Attenuated Total Reflectance (ATR) auxiliary, armed with crystal-diamond chamber. Isotherms from adsorption-desorption of nitrogen; surface area and samples porosity were counted at 77 K by Quantachrome Surface Autosorb-6B sorption analyzer. Mesoporosity was measured using Barret-Joyner-Halenda (BJH) model. Pre-treatment was carried out consistently at 523 K for 16 h. Total acidity was determined via ammonia temperature-programmed desorption (NH$_3$-TPD) using Micromeritics TPD 2900 in the temperature ranging from 300–1073 K subsequent to 3 progressive saturation measures at 473 K by means of purely ammonia. The types of acidities generated by the samples were determined using FTIR method by means of pyridine acting as probing agent. An own-supported wafer was affianced inside an *in situ* IR holder with CaF$_2$ windows. The samples were pre-heated for 1 h at 573 K within vacuum conditions to eliminate the feasible humidity and organic contaminants at the sample exterior. Successively, pyridine (10 Torr) was adsorbed on the actuated samples for 15 min at 423 K, subsequently degassing at 573 K. The IR spectra were documented within ambience circumstance at the vibrational region of pyridine (1400–1600 cm^{-1}) via Nicolet iS10 spectrometer. Transmission electron microscopy (TEM) imageries were achieved via JEOL JEM-2011 electron microscope armed with a Gatan 794 CCD camera and performed at 200 kV.

2.3. Oxidative catalytic performance

Epoxidation of olefins was performed via a glass sample vessel with sealant at ambient condition of 298 K (figure 1). Three sorts of analytical-grade olefins from Merck were designated as model reactants, namely aliphatic 1-octene, 99%, cyclic cyclohexene, 99% and aromatic styrene, 99%. Olefin (10 mmol) was added to 5 ml of solvent acetonitrile (ACN) with 50 mg synthesized catalyst for every single catalytic reaction. H$_2$O$_2$ (30 mmol) as oxidant was subsequently added. The mixture was agitated at 2000 rpm for 24 h, centrifuged and filtered for attainment of product. The product acquired was scrutinized via Shimadzu GC-2014 gas chromatography fitted FID sensor.
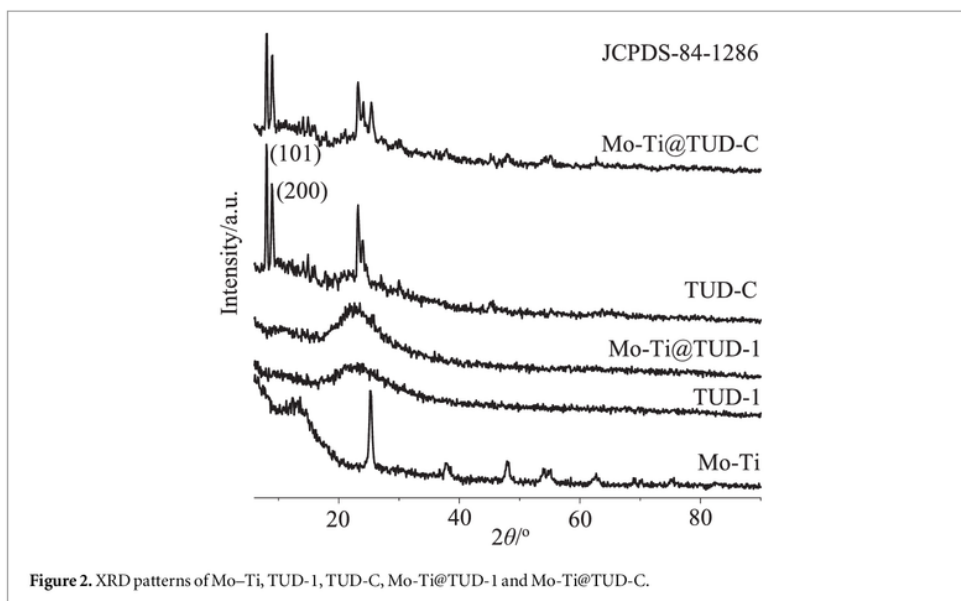
Figure 2. XRD patterns of Mo–Ti, TUD-1, TUD-C, Mo-Ti@TUD-1 and Mo-Ti@TUD-C.

The epoxides transformation and olefins selectivity were tabulated using the respective formulae:

$$X_S(\%) = \frac{[\text{conc. of olefins}]_{\text{beginning}} - [\text{conc. of olefins}]_{\text{ending}}}{[\text{conc. of olefins}]_{\text{beginning}}} \times 100\%$$

$$S_x(\%) = \frac{\text{formed epoxides peak area}}{\text{all formed products peak area}} \times 100\%$$

where X_S represents olefin conversion (%), S_x represents formed epoxides selectivity (%) formed through numerous olefins oxidation. Turnover number, TON and frequency, TOF of selected catalyst were tabulated using formulas as follow:

$$TON = \frac{\text{no. mol of product formed}}{\text{no. mol of reaction active sites}}$$

$$TOF = \frac{\text{turnover number (TON)}}{\text{duration of reaction}}$$

3. Results and discussion

3.1. Physical properties and characterization

Mo–TiO$_2$ is greyish powder whereas TUD-1 and TUD-C are white fine-powdery samples. Once Mo–Ti was loaded onto TUD-1 and TUD-C, all samples persisted as white powdery samples. As can be observed in figure 2, Mo–Ti formed anatase phase crystal structure which is well matched with reference JCPDS-84–1286. TUD-1 and Mo–Ti@TUD-1 displayed wide-ranging amorphous halo approximately at $2\theta = 20°-30°$, signifying the amorphous nature of the substances. In the meantime, TUD-C showed XRD array comparable to MFI phase crystal that was fitted to the commercially accessible ZSM-5 zeolite [17]. The two low angle characteristic peaks with indexing (101) and (200) acted as foremost sign for the MFI framework zeolitic structure formation integrated within disordered silicate structure. Expectantly, Mo–Ti@TUD-C sample exhibited mutually the distinctive anatase crystal phase with peak at $2\theta = 25.5°$ and TUD-C signature peaks, supportively signifying efficacious Mo–Ti integration within TUD-C.

Results obtained via Scherrer's formula detailed that the expansion of crystallite size ranging from 35 to 82 nm for Mo–Ti@TUD-C sample. The growth in crystallite size could be ascribed to the efficacious assimilation of Mo–Ti within the structure of TUD-C. The statement could be made plain due to the latent particulate development via the existence of additional silica [18]. It is commonly accredited that well crystallined structure expedites efficient reactants diffusion, whereas small crystalline particle was favourable for immense surface area, subsidizing the superior catalyst performance [19]. Thus, recent discoveries proposed where TUD-C with
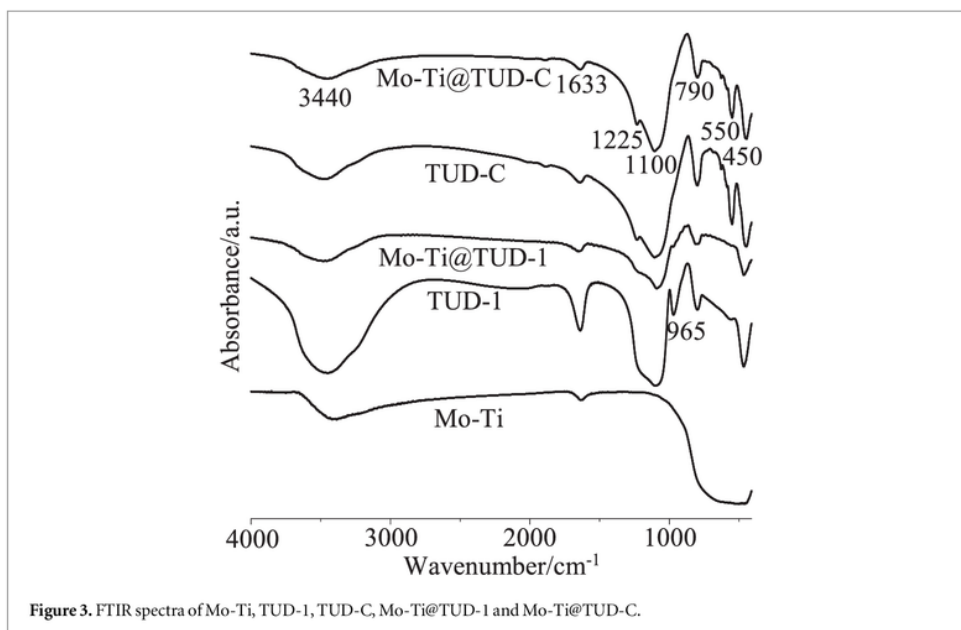
Figure 3. FTIR spectra of Mo-Ti, TUD-1, TUD-C, Mo-Ti@TUD-1 and Mo-Ti@TUD-C.

Si/Al ratio of 10 is optimal as it features the utmost crystalline structure with the tiniest crystalline structure conferring to preceding report [20].
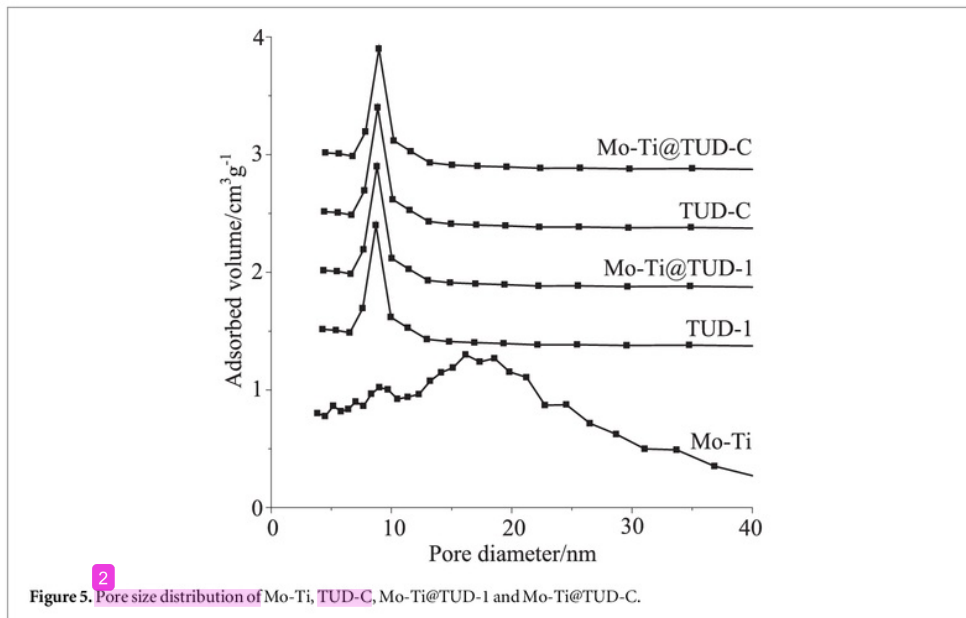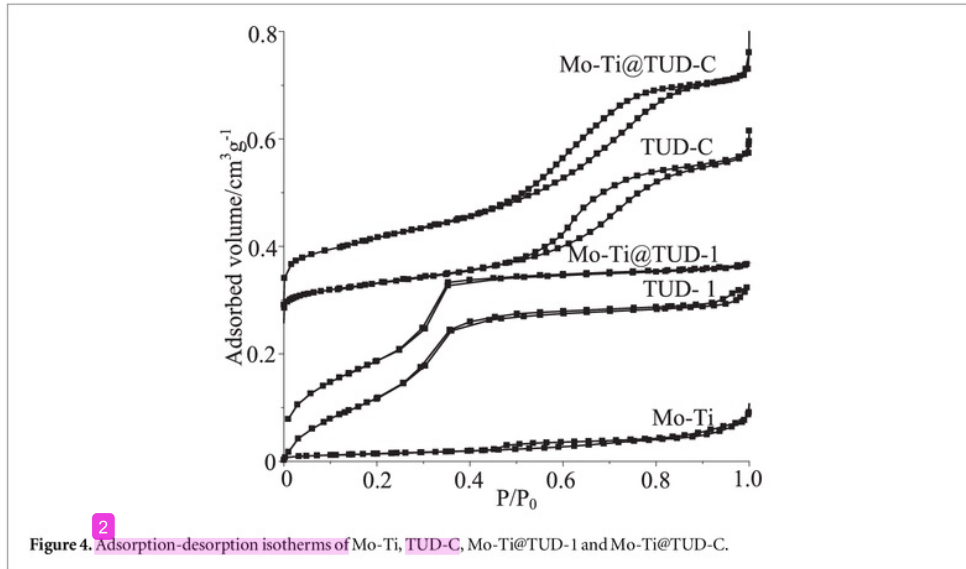
FTIR spectra (figure 3) illustrate the functional groups of Mo–Ti, TUD-1, TUD-C, Mo–Ti@TUD-1 and Mo–Ti@TUD-C. Sample Mo–Ti displayed an extensive peak within area 450–800 cm^{-1} because of superimposing Ti–O–Ti peak positioned at 150 cm^{-1} and Ti–OH peak, correspondingly. The peak at about 3400 cm^{-1} is appointed to OH (stretching) and 1633 cm^{-1} is corresponded to OH (bending). Meanwhile, TUD-C showed idiosyncratic ZSM-5 zeolitic peaks (T–O bending) at 450 cm^{-1}, vibration of MFI skeletal at 550 cm^{-1}, exterior Si–O–Si symmetrical stretching at 790 cm^{-1} and interior Si–O–Si symmetrical stretching at 1100 cm^{-1}. The external bonding (between TO$_4$ tetrahedral) at 1225 cm^{-1} performed as a complementary indication for the incidence of zeolitic structure of ZSM-5 which is indiscernible for all TUD-1 samples [9].

After loading of Mo–Ti, the zeolitic bonding strengths decline devoid of any substantial peak shifting, suggesting discomposure of the silicate linkage because of feasible Si–O–Ti and Si–O–Mo connections. The aforementioned recounted that the Si–O–Ti and Si–O–Mo bond linkages may well be proven thru the reduction of peak strength and peak shifting at 965 cm^{-1} which is connected to bending of Si–OH variants [21]. Such as illustrated in figure 3, the 965 cm^{-1} band was practically overlain by the wide band of 1100 cm^{-1} and look as if a small hump. Hence, whichever shifting occurred was unnoticeable. This alteration is apparent for the TUD-1 samples, after Mo–Ti was loaded on TUD-1, the peak intensity at 965 cm^{-1} was diminished for TUD-1 sample.

N$_2$ adsorption-desorption isotherms of Mo-Ti, TUD-1, TUD-C, Mo-Ti@TUD-1 and Mo-Ti@TUD-C are displayed in figure 4. At P/P$_0$ range between 0.05 to 0.45; all the samples established an isotherm with a virtually undeviating uptake, suggesting presence of minuscule mesoporous adjoining microporous within the samples. The application of TEAOH within the synthesis procedure has executed as a structural guiding component for all samples as it operated as the templating material for microporous development within MFI zeolitic framework assisted by autoclave at 403 K [22]. Moreover, TEAOH also proceeded as scaffold substance for establishment of mesostructure thru aging approach by ambient condition. During P/P$_0$ > 0.45, Mo–Ti demonstrated extremely tapered hysteresis loop. Contrariwise, TUD-1, TUD-C and every supported Mo–Ti samples revealed an isotherm with stepwise shifting uptake between P/P$_0$ at 0.45 to 0.85 showed isotherm of type IV with H1 hysteresis loop for all TUD-C samples, all TUD-1 samples presented an isotherm with mixture of type II/IV and H3 hysteresis loop that is sufficiently indicating the mesoporosity presented [23].

Together with the parallel plots of BJH pore size dissemination (figure 5), TUD-1, TUD-C and whole supported Mo–Ti samples exhibited a strident and fine dispersal of porosity with a middling 8.1 nm mesopores. Contrariwise, Mo–Ti displayed a widespread dispersal of porosity ranging from 10 to 30 nm.

As represented in table 1, Mo–Ti has the lowest surface area (162 m^2 g^{-1}) and pore volume (0.04 cm^3 g^{-1}). On contrary, TUD-C featured the utmost surface area (1451 m^2 g^{-1}) and pore volume (0.73 cm^3 g^{-1}). Both surface area and the porous capacity of TUD-1 and TUD-C decreased considerably once supported of Mo-Ti, inferring that a share distribution of Mo–Ti nanoparticles inside pores of TUD-1 and TUD-C. The annotations

Figure 4. Adsorption–desorption isotherms of Mo-Ti, TUD-C, Mo-Ti@TUD-1 and Mo-Ti@TUD-C.

Figure 5. Pore size distribution of Mo-Ti, TUD-C, Mo-Ti@TUD-1 and Mo-Ti@TUD-C.

Table 1. Surface area pore volume and pore diameter of Mo-Ti, TUD-1, TUD-C, Mo-Ti@TUD-1 and Mo-Ti@TUD-C.

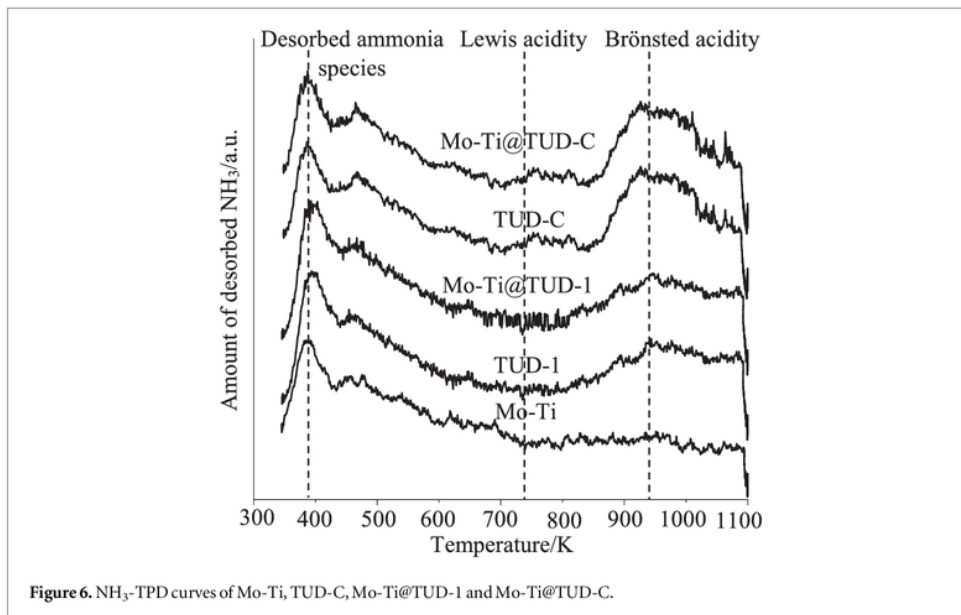| Sample	Surface area $(m^2\,g^{-1})$	Pore volume $(cm^3\,g^{-1})$	Pore diameter (nm)
Mo-Ti	162	0.04	9.82
TUD-1	924	0.69	2.83
Mo-Ti@TUD-1	864	0.57	3.44
TUD-C	1451	0.73	2.96
MoTi@TUD-C	1034	0.64	3.31

Figure 6. NH$_3$-TPD curves of Mo-Ti, TUD-C, Mo-Ti@TUD-1 and Mo-Ti@TUD-C.

Table 2. Overall acid sites amount of Mo-Ti, TUD-1, TUD-C, Mo-Ti@TUD-1 and Mo-Ti@TUD-C.

Sample	Quantity (mmol g^{-1})
Mo-Ti	0.120 54
TUD-1	0.158 02
Mo-Ti@TUD-1	0.182 47
TUD-C	0.257 68
Mo-Ti@TUD-C	0.340 36

remained wholly agreed with XRD outcomes, validating transformation of TUD-C well-arranged crystal structure to diminished crystal phase via loading of Mo–Ti as shown in figure 2.

Mo-Ti@TUD-C featured greater surface area (1034 m^2 g^{-1}), that was 6.4 times greater compared to Mo-Ti. Meanwhile, the diameter enlargement of porosity upon integration of Mo–Ti within TUD-1 and TUD-C, respectively could be ascribed to the deposition of Mo-TiO$_2$ alongside the pore opening and thus the increment of the pore width.

Figure 6 illustrates the spectra of temperature-programmed desorption by ammonia, NH$_3$-TPD for Mo-Ti, TUD-1, TUD-C, Mo-Ti@TUD-1 and Mo-Ti@TUD-C. As can be perceived in figure 6, sample Mo–Ti demonstrated an extensive desorption curvature by 346 K that anointed to NH$_3$ desorption from the acid sites, NH$_4^+$ + e → NH$_3$ [23]. There are inconsiderable changes detected after incorporation of Mo-TiO$_2$ within TUD-1. All supported TUD-1 samples persist as weakly acidic samples. Mo-Ti@TUD-C displayed additional expansive curve at 932 K that typically attributed as desorption of NH$_3$ from the Brønsted acidities [24]. An insipid desorption curve at 735 K allotted to Lewis acid sites was likewise perceived within sample. This statement was affably agreed to the aforementioned research claiming formation of mutually Brønsted and Lewis acidities in TUD-C, whilst alumina implement as proton donator (Brønsted acidity) with Si^{4+} acted as electron acceptor (Lewis acidity) [25]. The peak strength of Mo-Ti@TUD-C was affiliated to TUD-C, signifying the existing acidities within them were akin. Mo-Ti@TUD-C still continued a great rate of NH$_3$ desorption even further than 623 K, indicating vast acid strength of Mo-Ti@TUD-C. The outcomes demonstrated that the desorbed NH$_3$ capacity of Mo-Ti@TUD-C was sufficiently greater comparably to other samples as tabulated in table 2, suggesting higher concentration of acid sites within Mo-Ti@TUD-C and hence robust overall acid strength [26].

The acidity typing in all samples was further investigated using FTIR thru pyridine perform as probe reagent. FTIR spectra of the samples are illustrated in figure 7 at the pyridine vibrational state afterward pyridine adsorption and desorption for 15 min at 423 K. FTIR spectra presented adsorption peaks for Lewis acidity at
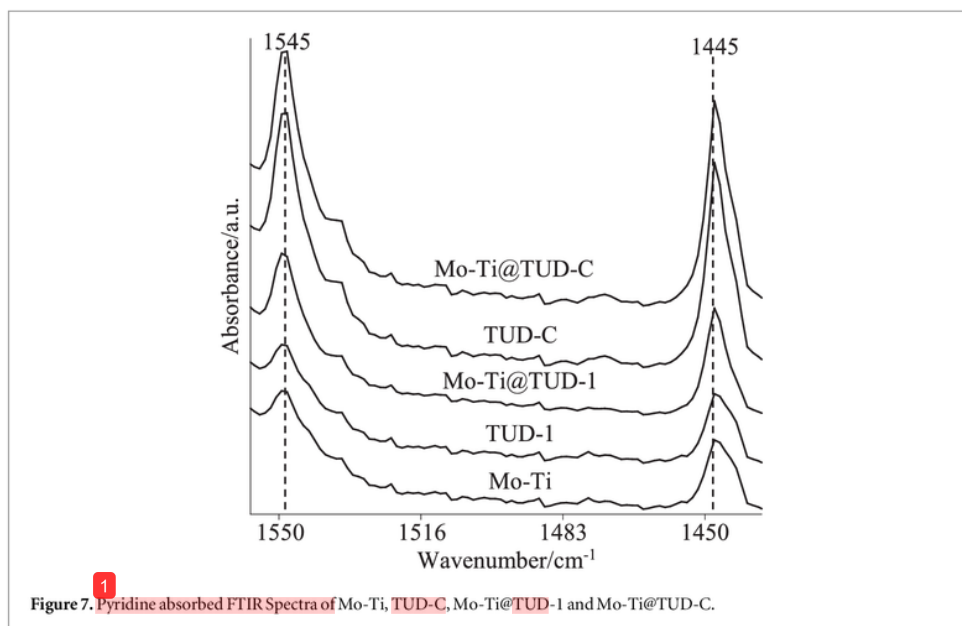
Figure 7. Pyridine absorbed FTIR Spectra of Mo-Ti, TUD-C, Mo-Ti@TUD-1 and Mo-Ti@TUD-C.

Table 3. The acidity amount in Mo-Ti, TUD-1, TUD-C, Mo-Ti@TUD-1 and Mo-Ti@TUD-C.

Sample	Acidity (μmol/g)	
	Lewis	Brønsted
Mo-Ti	6.7	2.1
TUD-1	7.1	2.5
Mo-Ti@TUD-1	7.6	3.1
TUD-C	19.1	13.3
Mo-Ti@TUD-C	17.9	12.9

1445 cm^{-1} and Brønsted acidity at 1545 cm^{-1}, correspondingly [15]. For all supported materials, the measure of Lewis (1445 cm^{-1}) and Brønsted acidities (1545 cm^{-1}) within samples was tabulated through the peak area separately.

  As demonstrated in table 3, TUD-C featured the utmost quantity of Brønsted acidities, trailed by Mo-Ti@TUD-C. This may possibly be elucidated thru manifestation of aluminosilicate sorts via the TUD-C structure, hence subsidizing to generation of advanced amount of Brønsted acidities. It was believed that the opposition between Mo–Ti and boundless Al_2O_3 has restrained generation of Brønsted acidities. Furthermore, Mo-Ti@TUD-C also displayed the utmost quantity of Lewis acidities, as represented in table 3. This occurrence advocated the plausible reaction among the Mo sorts and tetrahedral Ti kinds or straight with Si–O–Si within SiO_2 matrixes, which lead to higher development of Lewis acidities within samples. Transmission electron microscopy (TEM) analysis was carried out in the aforementioned report [15]. The calculated size of crystallite was relatively constant with that tabulated thru Scherrer's equation. Elemental conformations of the produced catalysts are displayed in table 4. It was perceived that all the elements presented within have a consistent dissemination.

3.2. Epoxidation of olefins

Catalytic valuation through several olefins epoxidation as archetypal reaction was evaluated. Three olefin sorts involving 1-octene, cyclohexene and styrene were designated as model reagents. Table 5(a)–(c) tabulates the yield, transformation and selectivity for corresponding alkenes tested using synthesized catalyst. For the 1-octene epoxidation, TUD-C catalyzed reaction only generated 10.7% conversion with 0.43 mmol of 1,2-epoxyoctane. On the other hand, insignificant quantity of 1,2-epoxyoctane was generated with Mo–TiO_2, TUD-1 or Mo-TiO_2/TUD-1 as the employed catalyst for the epoxidation. This is because of the immense inertness of

Table 4. The EDX elemental analysis of Mo-Ti, TUD-1, TUD-C, Mo-Ti@TUD-1 and Mo-Ti@TUD-C.

Samples	Atomic percentage (%)				
	Mo	O	Ti	Si	Al
Mo-Ti	15.87	51.57	32.56	—	—
TUD-1	—	47.41	—	52.59	—
Mo-Ti@TUD-1	0.14	43.30	13.25	43.31	—
TUD-C	—	54.09	—	45.55	0.36
Mo-Ti@TUD-C	0.17	41.77	11.88	45.91	0.27

Table 5. (a). Product yield, conversion and selectivity of epoxidation of 1-octene using Mo-Ti, TUD-1, TUD-C, Mo-Ti@TUD-1 and Mo-Ti@TUD-C. (b). Product yield, conversion and selectivity of epoxidation of cyclohexene using Mo-Ti, TUD-1, TUD-C, Mo-Ti@TUD-1 and Mo-Ti@TUD-C. (c). Product yield, conversion and selectivity of epoxidation of styrene using Mo-Ti, TUD-1, TUD-C, Mo-Ti@TUD-1 and Mo-Ti@TUD-C.

Catalyst	1,2-epoxyoctane (mmol)	Conversion (%)	Selectivity towards 1,2-epoxyoctane (%)
(a)			
Mo-Ti	—	—	—
TUD-1	—	—	—
Mo-Ti@TUD-1	—	—	—
TUD-C	0.43	4.3	100
Mo-Ti@TUD-C	2.70	27.0	100

Catalyst	1,2-epoxycyclohexane (mmol)	Conversion (%)	Selectivity towards 1,2-epoxycyclohexane (%)
(b)			
Mo-Ti	0.35	12.6	57
TUD-1	—	—	—
Mo-Ti@TUD-1	0.51	18.2	62
TUD-C	2.59	25.9	100
Mo-Ti@TUD-C	4.80	48.0	100

Catalyst	Styrene oxide (mmol)	Conversion (%)	Selectivity towards styrene oxide (%)
(c)			
Mo-Ti	1.07	21.0	67
TUD-1	—	—	—
Mo-Ti@TUD-1	1.25	27.6	74
TUD-C	3.70	37.0	100
Mo-Ti@TUD-C	6.20	62.0	100

the TUD-1 substance. Considerable yield boost of 12.8 times with conversion of 27% and complete selectivity headed for 1,2-epoxyoctane was attained through employing Mo-Ti@TUD-C catalyst in 1-octene epoxidation. Equivalent statement was observable for cyclohexene as stated in table 5(b) and styrene in table 5(c). As listed in tables 5(b), 1,2-epoxycyclohexane (4.8 mmol) with conversion of 48% and complete selectivity was pertained with the usage of Mo-Ti@TUD-C. Upsurge in yield was 11-times comparative to only Mo-Ti. For styrene epoxidation (table 5(c)), styrene oxide (6.2 mmol) with 8-times increment and conversion of 62% with complete selectivity was perceived.

TUD-C utilized as catalytic supporting material has improved the selectivity from ~57 to 100% for every types of olefins epoxidation. Enhanced selectivity of TUD-C and TUD-C supporting catalysts may possibly be attributed to mesoporosity (2.96–3.31 nm pore size) with fine porosity dissemination of the catalysts. Amidst, for epoxidation of olefins, Mo–Ti was the most unassuming catalyst. Previous report stated that Mo doped TiO_2 performed as effective, non-selective catalyst with incidence of H_2O_2 [27]. Reaction amid transition metals oxide with H_2O_2 produced ·OH radicals that were requisite for olefins epoxidation via separation of peroxo-metal sorts [28]. Conversely, Paolo *et al.* revealed that hydroxylated Al_2O_3 were remarkably discerning for numerous olefins epoxidation. Recommended catalytically active array included generation of peripheral hydroperoxide aluminium variants, Al–OOH from the reaction between exterior hydroxyl aluminium sorts, Al–OH and H_2O_2 [29]. Present research proposed that Al_2O_3 could possibly occur as free-bound Al_2O_3 and Al existed in TUD-C aluminosilicate framework and Mo-Ti@TUD-C catalysts. These Al variants were estimated to perform a

Table 6. TON and TOF of Mo-Ti@TUD-C catalyst in epoxidation of various olefins.

Olefin	TON	TOF/h^{-1}
1-octene	43.13	1.80
Cyclohexene	76.67	3.19
Styrene	99.03	4.13

Table 7. TON and TOF of Mo-Ti@TUD-1 catalyst in epoxidation of various olefins.

Olefin	TON	TOF/h^{-1}
1-octene	0.48	0.02
Cyclohexene	18.72	0.78
Styrene	37.20	1.55

substantial part in the epoxidation of olefins after reaction with H_2O_2. On the other hand, the catalytic competency of TUD-C was related to the Brønsted acidities within samples as zeolites and zeolitic matters were comprehensively accounted as superior catalysts [30]. The contemporary outcomes validated that Mo-Ti@TUD-C was superior for the epoxidation of olefins paralleled to other tried catalysts. The outstanding catalytic performance of Mo–Ti supported on TUD-C was accredited to the synergistic outcome between Mo–Ti and TUD-C. The mesoporosity of TUD-C had diminished the zeolitic constricting effect [31]. Consequently, shape selectivity was improved and the bulky reactants could come into contact with the available active sites at ease on molybdena doped titania via mesoporous zeolitic passage, without problem of pore obstruction. In addition, TUD-C supporting catalysts with high surface area might possibly be assisted the uniform dispersal of the active species onto the support's surface which aided the adsorption of reactant molecules at active sites, resulted increment in catalytic performance. Additionally, the enhanced crystallinity had assisted the reactant's diffusivity. Perceivably, catalytic performance was proportionally related to catalyst's crystallinity. The cohabitation of Brønsted and Lewis acidities seemed to be an alternative essential influence for enhanced catalytically active Mo-Ti@TUD-C catalyst.

Conferring to Next Nearest Neighbor Theory [32], optimum ratio between Brønsted and Lewis acidities is vital for establishing superior catalytic activity. The substance appeared as catalytically sedentary if featured Brønsted or Lewis acidities only [33]. The comparatively insipid performance of Mo-Ti, TUD-1 and Mo-Ti@TUD-1 would be attributed to minimal acidities with absence of efficacious active sites for epoxidation. Among the three olefins, Mo-Ti@TUD-C most highly fitted for styrene epoxidation (6.2 mmol of styrene oxide), subsequently cyclohexene (4.8 mmol of 1,2-epoxycyclohexane), with slightest suitability for 1-octene epoxidation (2.7 mmol of 1,2-epoxyoctane). Tables 6 and 7 tabulate the turnover amount, TON and turnover rate, TOF of Mo-Ti@TUD-C and Mo-Ti@TUD-1, respectively.

Mo-Ti@TUD-C attained the highest TON at 99.03 and TOF at 4.13 h^{-1}, respectively for styrene epoxidation. After reaction with Brønsted acidities within TUD-C, styrene was estimated to generate highly steady carbo-cation due to existence of electron donor (phenolic group). Delocalized electrons were offered to adjoining carbon forming the conjugating carbon. In the meantime, cyclohexene formed the next steady carbo-cation because of neighboring 2 methylene variants that performed as electron donors. 1-octene produced the carbo-cation with the lowest stability allotted to the end-chain double bonding that features mono alkyl sort only [34]. Additionally, Mo–Ti was alleged having reaction with H_2O_2 for the formation of peroxospecies that is essential for the formation of hydroxyl radical [35]. The reaction amid ·OH radical and generated carbo-cations formed numerous epoxides as final yield. The epoxides formed trailed the descendent inclination of styrene oxide >1,2- epoxycyclohexane >1,2-epoxyoctane conferring to the preceding report. First order kinetic which solely reliant on the reactants was determined for numerous olefins epoxidation was acquired from previous research. Akin kinetics conduct was accounted from literature during employment of metal oxide catalyst for epoxidation of olefins [15].

4. Conclusion

Results presented the remarkable enhancement of Mo–Ti catalytic activity in epoxidation enhanced remarkably subsequently supported onto TUD-1 and TUD-C respectively. Between TUD-C and TUD-1, TUD-C supported

catalysts have shown significantly higher yield and selectivity compared to those of supported on TUD-1. The high acidity amount in TUD-C could be crucial for the improved performance. Fine dissemination of hierarchical mesoporous within TUD-C supported materials and existence of highly active zeolitic material subsidized the 100% selectivity headed formation of epoxides. Amongst, Mo-Ti@TUD-C was the utmost proficient epoxidative catalyst for 3 different olefins at room temperature. The research findings strongly indicated TUD-C is a better support for Mo–Ti oxidative catalyst for numerous sorts of olefins epoxidation.

Acknowledgments

ORCID iDs

Leny Yuliati ⓘ https://orcid.org/0000-0003-1600-5757
Siew Ling Lee ⓘ https://orcid.org/0000-0002-7325-0321

References

[1] Zietzschmann F, Mitchell R L and Jekel M 2015 *Water Res.* **84** 153–60
[2] Zhang S, Li X-S, Zhu B, Liu J-L, Zhu X, Zhu A-M and Jang B W L 2015 *Catal. Today.* **256 Part 1** 142–7
[3] Zhou K, Xie X D, Chang C T, Xue N and Hou W 2017 *Appl. Surf. Sci.* **416** 248–58
[4] Lee S L and Hamdan H J 2008 *Non-Crystalline Solids* **354** 3939–43
[5] Pourdayhimi P, Koh P W, Salleh M M, Nur H and Lee S L 2016 *Aust. J. Chem.* **6** 790–7
[6] Zhai Z, Wang X, Licht R and Bell A T 2015 *J. Catal.* **325** 87–100
[7] Yeung K L and Han W 2014 *Catal. Today.* **236 Part B,** 182–205
[8] Ye J, Li X, Hong J, Chen J and Fan Q 2015 *Mater. Sci. Semicon. Process.* **39** 17–22
[9] Wang Y, Xue X and Yang H 2014 *Cera. Int.* **40** (**8, Part A)** 12533–7
[10] Ye D, Qu R, Song H, Gao X, Luo Z, Ni M and Cen K 2016 *Chem. Eng. J.* **283** 846–54
[11] Zhou J, Hua Z and Shi J 2009 *Chemistry A European Journal* **15** (47) 12949–54
[12] Yamamoto T, Yasuhara A, Shiraishi H and Nakasugi O 2001 *Chemosphere* **42** 415–8
[13] Xu Q, Järn M, Lindén M and Smått J-H 2013 *Thin Solid Films* **531** 222–7
[14] Ooi Y K, Yuliati L and Lee S L 2016 *Chinese J. Catal.* **37** 1871–81
[15] Ooi Y K, Yuliati L, Hartanto D, Nur H and Lee S L 2016 *Micro. Meso. Mater.* **225** 411–20
[16] Ooi Y K, Yuliati L and Lee S L 2014 *Jurnal Teknologi* **69** 81–6
[17] Wu G, Koliadima A, Her Y-S and Matijević E 1997 *J, Col. Int. Sci.* **195** 222–8
[18] Wong C L, Tan Y N and Mohamed A R J 2011 *Environ. Manage.* **92** 1669–80
[19] Witt P M, Somasi S, Khan I, Blaylock D W, Newby J A and Ley S V 2015 *Chem. Eng. J.* **278** 353–62
[20] Wickramaratne N P and Jaroniec M J 2015 *Col. Int. Sci.* **449** 297–303
[21] Wang X, Gao X, Dong M, Zhao H and Huang W J 2015 *Energy. Chem.* **24** 490–6
[22] Wang J-J, Xie J-R, Huang Y-H, Chen B-H, Lin G-D and Zhang H-B 2013 *Appl. Catal. A: General.* **468** 44–51
[23] Wang J, Yue W, Zhou W and Coppens M-O 2009 *Micro. Meso. Mater.* **120** 19–28
[24] Wang G, Chen S, Yu H and Quan X J 2015 *Hazard. Mater.* **299** 27–34
[25] Tungatarova S A, Abdukhalykov D B, Baizhumanova T S, Komashko L V, Grigorieva V P and Chanysheva I S 2015 *Catal. Today.* **256 Part 2** 276–86
[26] Tshabalala T E, Coville N J and Scurrell M S 2014 *Appl. Catal. A: General.* **485** 238–44
[27] Tsai J-K, Meen T-H, Wu T-C, Lai Y-D and He Y-K 2015 *Micro. Eng.* **148** 55–8
[28] Thalluri S M, Hernández S, Bensaid S, Saracco G and Russo N 2016 *Appl. Catal. B: Environ.* **180** 630–6
[29] Suresh D, Udayabhanu N H and Sharma S C 2015 *Mater. Let.* **142** 4–6
[30] Srinivasan V V, Ramanathan A, Maheswari R, Imran G, Rajalakshmi R and Nilamadanthai A 2015 *Mater. Res. Bulletin* **70** 914–9
[31] Song Y, Liang S, Li F, Wang X, You C and Yang Y 2015 *Mater. Let.* **161** 100–3
[32] Shan Z, Jansen J C, Marchese L and Maschmeyer T 2001 *Micro. Meso. Mater.* **48** 181–7
[33] Shams-Ghahfarokhi Z and Nezamzadeh-Ejhieh A 2015 *Mater. Sci. Semicon. Process* **39** 265–75
[34] Sachse A, Wuttke C, Díaz U and de Souza M O 2015 *Micro. Meso. Mater.* **217** 81–6
[35] Phung T K, Proietti H L, Lagazzo A and Busca G 2015 *Appl. Catal. A: General* **493** 77–89
[36] Koh P W, Yuliati L, Lintang O H and Lee S L 2015 *Aust. J. Chem.* **68** 1129–35
[37] Khang K C L, Hatta M H M, Lee S L and Yuliati L 2018 *Jurnal Teknologi* **8** (2) 153–60
[38] Zhang L, He Y, Yang X, Yuan H, Du Z and Wu Y 2015 *Chem. Eng. J.* **278** 129–33

MRE2019_2

1   hadinur.com
Internet Source   **5**%

2   Yee Khai Ooi, Leny Yuliati, Djoko Hartanto, Hadi Nur, Siew Ling Lee. "Mesostructured TUD-C supported molybdena doped titania as high selective oxidative catalyst for olefins epoxidation at ambient condition", Microporous and Mesoporous Materials, 2016
Publication   **5**%

3   link.springer.com
Internet Source   **1**%

4   N F Ghazalli, L Yuliati, H O Lintang. "Molecular Self-Assembly of Group 11 Pyrazolate Complexes as Phosphorescent Chemosensors for Detection of Benzene", IOP Conference Series: Materials Science and Engineering, 2018
Publication   **1**%

5   Ooi, Yee Khai, Leny Yuliati, Djoko Hartanto, Hadi Nur, and Siew Ling Lee. "Mesostructured   **1**%

TUD-C supported molybdena doped titania as high selective oxidative catalyst for olefins epoxidation at ambient condition", Microporous and Mesoporous Materials, 2016.
Publication

6   Kamanashis Sarkar, Krishna Deb, Arun Bera, Ajit Debnath, Biswajit Saha. "Tuning of optical and electrical properties of polyaniline on flexible cellulose through Eosin Y dye interaction", Materials Research Express, 2019
Publication

1%

7   Yee Khai Ooi, Leny Yuliati, Siew Ling Lee. "Phenol photocatalytic degradation over mesoporous TUD-1-supported chromium oxide-doped titania photocatalyst", Chinese Journal of Catalysis, 2016
Publication

1%

8   Tang, H.. "Cu-incorporated mesoporous materials: Synthesis, characterization and catalytic activity in phenol hydroxylation", Journal of Molecular Catalysis. A, Chemical, 20061215
Publication

<1%

9   Leny Yuliati, Peggy Tiong, Hendrik O Lintang. "Response surface methodology to optimize the performance of reduced graphene oxide-mesoporous carbon nitride photocatalysts",

<1%

Materials Research Express, 2019
Publication

10 Marler, B.. "Synthesis and structure of RUB-35, a disordered material of the EUO-NES-NON family", Microporous and Mesoporous Materials, 20031003
Publication

<1%

11 Tingjun Fu, Jiangwei Chang, Juan Shao, Zhong Li. "Fabrication of a nano-sized ZSM-5 zeolite with intercrystalline mesopores for conversion of methanol to gasoline", Journal of Energy Chemistry, 2017
Publication

<1%

12 Submitted to University of Western Australia
Student Paper

<1%

13 Ling, L.S.. "Sulfated silica-titania aerogel as a bifunctional oxidative and acidic catalyst in the synthesis of diols", Journal of Non-Crystalline Solids, 20080901
Publication

<1%

14 doc.uments.com
Internet Source

<1%

15 Submitted to Universidade Estadual de Campinas
Student Paper

<1%

16 Submitted to Gaziantep Aniversitesi
Student Paper

<1%

17   Xiong, Haifeng, Linda L. Jewell, and Neil John Coville. "Shaped carbons as supports for the catalytic conversion of syngas to clean fuels", ACS Catalysis

Publication

<1%

18   Submitted to Universiti Malaysia Pahang

Student Paper

<1%

19   sevgiligiyim.com

Internet Source

<1%

Exclude quotes	Off	Exclude matches	Off
Exclude bibliography	On		